Multipole, nonlinear, and anharmonic uncertainties of clocks of Sr atoms in an optical lattice

V. D. Ovsiannikov
Physics Department, Voronezh State University, Voronezh 394006, Russia

V. G. Pal'chikov
Institute of Metrology for Time and Space at National Research Institute for Physical-Technical and Radiotechnical Measurements, Mendeleevo, Moscow Region, 141579, Russia

A. V. Taichenachev and V. I. Yudin
Institute of Laser Physics SB RAS, pr. Ac. Lavrentyeva, 13/3, Novosibirsk, 630090 Russia, Novosibirsk State University, ul. Pirogova, 2, Novosibirsk, 630090, Russia, Novosibirsk State Technical University, pr. K. Marksa, 20, Novosibirsk, 630073, Russia, and Russian Quantum Center, Skolkovo, Moscow Reg., 143025, Russia

Hidetoshi Katori
Department of Applied Physics, Graduate School of Engineering, The University of Tokyo, Bunkyo-ku, Tokyo 113-8656, Japan, Innovative Space-Time Project, ERATO, Japan Science and Technology Agency, Bunkyo-ku, Tokyo 113-8656, Japan and Quantum Metrology Laboratory, RIKEN, Wako-shi, Saitama 351-0198, Japan

(Received 19 April 2013; published 8 July 2013)

Magnetic-dipole, electric-quadrupole, and hyperpolarizability effects on clock energy levels are analyzed in detail for Sr atoms in Stark potentials of red-detuned and blue-detuned magic-wavelength optical lattices. A difference between ac Stark shifts in traveling and standing waves is determined numerically. Differences between magic wavelengths for atoms in traveling and standing waves are presented and strategies for minimizing uncertainties of the clock frequency are indicated explicitly. Significant suppression of hyperpolarizability effect is demonstrated analytically for a blue-detuned in comparison with a red-detuned lattice, thus enabling essential deepening of trap potentials, reducing tunneling between lattice wells and collision effects.

DOI: 10.1103/PhysRevA.88.013405 PACS number(s): 37.10.Jk, 42.50.Gy, 42.62.Fi, 42.62.Eh

I. INTRODUCTION

Recent years have seen essential achievements in the field of high-precision laser spectroscopy based on simultaneous interrogation of strongly forbidden optical transitions in a large number of alkaline-earth-like atoms, confined to an optical lattice at the magic wavelength (MWL). In addition to well-studied fermionic and bosonic Sr atoms [1–4], the MWL and corresponding optical properties were well defined for Yb and Hg atoms [5,6]. The use of clock transitions was also discussed for creation of a millihertz-linewidth laser [7].

The progress in designing atomic optical frequency standards with unprecedented fractional frequency uncertainty at a level of 10^{-18} requires unprecedented accuracy in estimating the role of different sporadic and stray-field effects [8]. In particular, an accurate control of the shift induced by blackbody radiation (BBR) is possible by the on-site measurement of the BBR temperature with a mK precision at usual laboratory conditions [9], or by the use of the "synthetic" frequency spectroscopy free of BBR shift [10]. Two recent works [11,12] have presented experimental and theoretical data on the BBR-induced shift of the clock frequency in Sr atoms, which enable a high-precision account of the effect at room temperature, reducing the temperature-related clock uncertainties to the level below 10^{-17}.

However, more important effects on uncertainties should be clarified in more detail, in particular those related with the definition and precision of the MWL, as the wavelength providing atomic-motion-insensitive conditions for the frequency of clock transition [13]. To this end, the role of higher-order and multipole atom-lattice interaction in the definition of the MWL should be considered. The anharmonic effects on vibrational motion of atoms inside the lattice should be also taken into account as the precision-restricting factors, introducing some difference between the motions of atoms trapped into the lattice potential wells in upper (excited) and lower (ground) clock states. Therefore, corresponding limitations may arise for spectroscopy of atoms confined to an optical lattice of a MWL. In particular, the response should be given to the following questions.

(i) What ranges of uncertainties for the MWL may be acceptable to ensure equality and atomic-motion independence of the Stark shifts for upper and lower clock states, sufficient to reduce the clock uncertainties at the level of 10^{-18}?

(ii) What is the difference between the effective Stark shifts of the clock frequencies in traveling and standing laser waves and does it influence on the definition of the MWL?

(iii) What is the influence of higher-order and multipole effects on clock levels in a standing wave?

(iv) What is the difference between uncertainties on clock frequencies in red-detuned (attractive) and blue-detuned (repulsive) optical lattices?

These problems were already studied and discussed in part in Refs. [13–15]. Preliminary numerical estimates of E2 and M1 polarizability and hyperpolarizability effects were presented for red-detuned MWL in Ref. [16] and for blue-detuned MWL in Refs. [13,14]. The influence of higher-

order (hyperpolarizability) effects on the lattice-based clock uncertainties was estimated theoretically [16,17] and measured experimentally [18,19] for Sr and Yb atoms trapped in MWL lattices. In the lattices with red-detuned MWL the higher-order Stark-shift uncertainties were determined at the level of 10^{-17} [2] and therefore were put aside for further considerations.

Meanwhile, the target uncertainties at the level of 10^{-18} require more and more precise estimates of the lattice-atom interaction effects with account of inhomogeneity of the lattice field spatial distribution. The indicated effects cause unavoidable systematic shifts of the clock frequency, which should be correctly controlled (compensated or taken into account) in high-precision laser spectroscopy measurements.

In this article, we present detailed analysis of linear in the laser intensity I clock-frequency shifts from multipole interactions (magnetic-dipole M1 and electric-quadrupole E2) and quadratic in I shifts (electric dipole hyperpolarizability effects) of the Sr atom clocks in both the red-detuned and blue-detuned optical MWL lattices.

The principal difference between red-detuned and blue-detuned lattices consists in the location of atomic occupancy sites. The Stark potential in the red-detuned lattice is attractive, so the potential minima locate in maxima of the lattice-wave electric-field amplitude. Thus, the optical lattice with the red-detuned MWL tends to confine atoms in the vicinity of the standing-wave antinodes. By contrast, the lattice with blue-detuned MWL repulses atoms to the standing-wave nodes, where electric-field amplitudes vanish. So, the lattice field effects on the clock frequency in the latter is significantly smaller than those in the former.

Electric-dipole forces provide the basic contribution to the atom-lattice interaction. Simple considerations demonstrate that to make the lattice-induced uncertainties of the clock frequency at the level of 10^{-18}, the fractional difference between E1 polarizabilities of the clock levels should not exceed 0.5×10^{-9} when the depth of lattice wells achieves 0.6 MHz. In these conditions, M1 and E2 effects, which are approximately seven orders smaller than the E1 effect, should be taken into account together with quadratic in the laser intensity I interactions, since their fractional contributions may impede reducing clock uncertainties to the target level.

The moderation of uncertainties from multipole and hyperpolarizability effects is restricted from below by the limitations on the laser intensity I, which should be sufficiently large for trapping atoms in vibrational states with negligibly small widths of tunneling between adjacent wells. To this end, the well depths U_0 and the energy of atomic vibrations Ω should exceed essentially the lattice photon recoil energy $\mathcal{E}^{\rm rec}$ [19,20] (atomic units $e = m = \hbar = 1$, with the speed of light $c = 137.036$ a.u., are used throughout this paper, unless otherwise specified explicitly),

$$U_0 \gg \Omega \gg \mathcal{E}^{\rm rec} = \frac{k^2}{2\mathcal{M}}, \tag{1}$$

where $k = \omega/c$ is the wave number of the lattice wave with the angular frequency ω, and $\mathcal{M}$ is the atomic mass. In view of so rigorous restrictions on the lattice-wave intensity from below, an accurate account of multipole, nonlinear, and anharmonic effects is the necessary condition for reducing the clock fractional uncertainties to the level of 10^{-18}.

We consider in detail the role of indicated effects on the clock transition in strontium atoms confined to an optical lattice of a MWL. All calculations were performed in the model-potential approximation, the uncertainties of which in evaluating electromagnetic transition amplitudes and susceptibilities of interaction with external fields for two-valence-electron atoms do not exceed 10% at most [21]. Numerical results are presented for lattices with red-detuned MWL $\lambda^r_m = 813.42727$ nm [2] and blue-detuned MWL $\lambda^b_m = 389.889$ nm [14]. Due to very strong dependence of hyperpolarizabilty on frequency, the data for now exactly known MWL differ considerably from those made for an approximately estimated value $\lambda^r_m \approx 800$ nm in Ref. [16].

Evidently, basic properties and principal features of one-dimensional (1D) lattices may be transferred to their superpositions in 2D and 3D lattices. Therefore, we confine ourselves to investigations of a 1D case.

II. ATTRACTIVE LATTICE POTENTIAL WITH A RED-DETUNED MWL

Position and time dependence of electric-field vector of a 1D lattice standing wave may be written as

$$\mathbf{E}(\mathbf{R},t) = 2E_0\mathbf{e}\cos(\mathbf{k}\cdot\mathbf{R})\cos(\omega t), \tag{2}$$

where E_0 is the scalar amplitude of the laser wave. The factor 2 accounts for the superposition of forward and backward traveling waves, which doubles the lattice standing-wave amplitude in comparison with that of the incident (forward traveling) laser radiation. This doubling corresponds to the four-times increase of the potential-well depths. $\mathbf{k} = \mathbf{n}\,\omega/c$ is the wave vector, $\mathbf{n}$, the unit wave vector; $\mathbf{e}$ is the unit polarization vector $\mathbf{e}\cdot\mathbf{e} = 1$ (linear polarization of the laser wave, $\mathbf{e} = \mathbf{e}^*$, is assumed here for simplicity). The plane-wave transversal condition $\mathbf{k}\cdot\mathbf{e} = 0$ holds also for the lattice wave. The position vector $\mathbf{R}$ originates in an antinode of the standing wave.

According to Maxwell's equation

$$\mathrm{curl}(\mathbf{E}) = -\frac{1}{c}\frac{\partial\mathbf{B}}{\partial t},$$

the magnetic field vector is

$$\mathbf{B}(\mathbf{R},t) = 2E_0[\mathbf{n}\times\mathbf{e}]\sin(\mathbf{k}\cdot\mathbf{R})\sin(\omega t). \tag{3}$$

As is seen from (2) and (3), the magnetic-dipole interaction, $\hat{V}_{M1} = -\mathbf{m}\cdot\mathbf{B}$, is a quarter wavelength out of phase with the electric-dipole E1 interaction $\hat{V}_{E1} = -\mathbf{d}\cdot\mathbf{E}$. The magnetic-dipole moment of atom is $\mathbf{m} = -(\mathbf{L} + 2\mathbf{S})/2c$, where $\mathbf{L}$ is the total angular momentum and $\mathbf{S}$, the total atomic spin; $\mathbf{d} = -\mathbf{r}$ is the electric-dipole moment.

Separating the position of atom from internal atomic variables, the operator of atom-lattice interaction may be presented as

$$\hat{V}(X,t) = \mathrm{Re}[\hat{V}(X)\exp(-i\omega t)], \tag{4}$$

where X determines the position of atomic nucleus along the standing-wave axis starting from the standing-wave antinode, the center of localization for the trapped atom. The spatial part of operator is given by

$$\hat{V}(X) = \hat{V}_{E1}\cos(kX) + (\hat{V}_{M1} + \hat{V}_{E2})\sin(kX). \tag{5}$$

The coefficients at cosine and sine functions here are the operators of E1, M1, and E2 atom-lattice interaction depending on only internal atomic variables. The outermost electrons provide principal contributions into amplitudes of the interactions, therefore in our numerical estimates we use a single-electron approximation where the operators may be presented as follows:

$$\hat{V}_{E1} = E_0(\mathbf{r}\cdot\mathbf{e}); \quad \hat{V}_{M1} = \frac{E_0}{2c}\{[\mathbf{n}\times\mathbf{e}]\cdot(\mathbf{L}+2\mathbf{S})\};$$
$$\hat{V}_{E2} = E_0\frac{\omega}{\sqrt{6}c}\,r^2\,[\{\mathbf{n}\otimes\mathbf{e}\}_2\cdot\mathbf{C}_2(\theta,\phi)]\,. \tag{6}$$

Here $\{\mathbf{n}\otimes\mathbf{e}\}_2$ is the rank 2 tensor product of the wave and polarization unit vectors, $\mathbf{C}_2(\theta,\phi)$ is the modified spherical function of the angular variables of the atomic electron position vector $\mathbf{r}=\{r,\theta,\phi\}$ [22]. The interaction (4) of a ground-state (excited) atom produces potential energy proportional to the laser intensity I, which equals to the second-order Stark shift:

$$U^{(2)}_{g(e)}(X) = -\left\{\alpha^{E1}_{g(e)}(\omega) - \alpha^{dqm}_{g(e)}(\omega)\sin^2(kX)\right\}I, \tag{7}$$

where

$$\alpha^{dqm}_{g(e)}(\omega) = \alpha^{E1}_{g(e)}(\omega) - \alpha^{qm}_{g(e)}(\omega) \tag{8}$$

is the difference between the electric dipole $\alpha^{E1}_{g(e)}(\omega)$ and the sum $\alpha^{qm}_{g(e)}(\omega)=\alpha^{M1}_{g(e)}(\omega)+\alpha^{E2}_{g(e)}(\omega)$ of magnetic-dipole and electric-quadrupole dynamic polarizabilities of a ground-state (g) [excited-state (e)] atom at the frequency of the lattice wave ω. Here and in all equations below I is the intensity of a single traveling laser wave. The intensity of the laser wave in the antinode is $4I$ [for explanation, see the text after Eq. (2)].

The fourth-order in operator (4) corrections to the clock-level energies determine quadratic in I Stark shifts of the lattice potential. With account of only the electric-dipole interaction from (5) it is described by the dipole dynamic hyperpolarizability $\beta_{g(e)}(\omega)$ of the ground (excited) state

$$U^{(4)}_{g(e)}(X) = -\beta_{g(e)}(\omega)I^2\cos^4(kX). \tag{9}$$

Resolving the sine and cosine functions in power series of their arguments and confining ourselves to harmonic ($\propto X^2$) and lowest-order anharmonic terms ($\propto X^4$), we get for the lattice potential an oscillatorlike form with coefficients depending on the lattice laser intensity up to I^2 terms

$$\begin{aligned} U^{L}_{g(e)}(X) &= U^{(2)}_{g(e)}(X) + U^{(4)}_{g(e)}(X) \\ &= -\alpha^{E1}_{g(e)}(\omega)I - \beta_{g(e)}(\omega)I^2 \\ &\quad + \left[\alpha^{dqm}_{g(e)}(\omega)I + 2\beta_{g(e)}(\omega)I^2\right](kX)^2 \\ &\quad - \left[\alpha^{dqm}_{g(e)}(\omega)I + 5\beta_{g(e)}(\omega)I^2\right]\frac{(kX)^4}{3}. \end{aligned} \tag{10}$$

The coefficient at X^2 may be equalized to $\mathcal{M}\Omega^2_{g(e)}/2$, where $\Omega_{g(e)}$ is the oscillator eigenfrequency. Correspondingly, the coefficient at X^4 may be written as $[\mathcal{M}\Omega^2_{g(e)}/6+\beta_{g(e)}(\omega)k^2I^2]k^2$. Averaging the Hamiltonian of trapped atom $\hat{\mathcal{H}}^L_{g(e)}(X)=\hat{P}^2/(2\mathcal{M})+U^L_{g(e)}(X)$ over positions in a vibrational state with a quantum number n, we get the vibrational energy $E^{\rm vib}_{g(e)}(I,n)$ of a ground-state (excited) atom

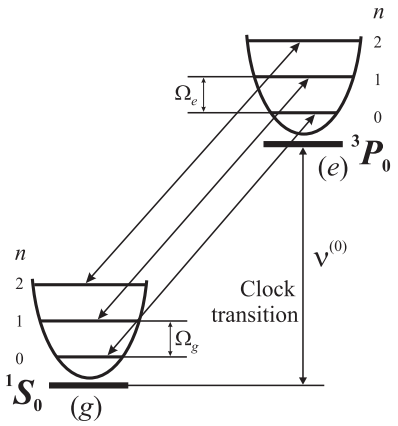

FIG. 1. An illustration of optical transitions between vibrational levels for atoms confined to an optical lattice.

(see Fig. 1)

$$\begin{aligned} E^{\rm vib}_{g(e)}(I,n) &= \langle n|\hat{\mathcal{H}}^L_{g(e)}(X)|n\rangle \\ &= -\alpha^{E1}_{g(e)}(\omega)I - \beta_{g(e)}(\omega)I^2 + \Omega_{g(e)}\left(n+\frac{1}{2}\right) \\ &\quad - \frac{\mathcal{E}^{\rm rec}}{2}\left[1+\frac{3\beta_{g(e)}(\omega)I}{\alpha^{dqm}_{g(e)}(\omega)}\right]\left(n^2+n+\frac{1}{2}\right). \end{aligned} \tag{11}$$

In averaging the anharmonic term, the relation is used

$$\langle n|X^4|n\rangle = \frac{3}{2}X_0^4\left(n^2+n+\frac{1}{2}\right),$$

where $X_0=(\mathcal{M}\Omega)^{-1/2}\propto I^{-1/4}$ is the oscillator length scaling factor. Therefore, the frequency Ω^2 in the coefficient at X^4 cancels out, leaving behind an intensity-independent term, proportional to the recoil energy $\mathcal{E}^{\rm rec}$ and quadratic in n polynomial. The quadratic in I part of the coefficient turns into the linear in I term.

It should be taken into account that the harmonic approximation for the motion of atom in the potential well (10) holds only if the anharmonic term in the last line of Eq. (11) is significantly smaller than the vibrational frequency $\Omega_{g(e)}$. It also means that the scaling factor X_0 should be significantly smaller than half-widths of wells in the lattice with the wavelength λ_m, which determines also the spacing between the lattice potential wells, $X_0\ll\lambda_m/4$. This inequality may be rewritten as $\sqrt{\mathcal{E}^{\rm rec}}\ll\sqrt{\Omega}$, thus strengthening the second inequality in (1).

The indicated conditions impose limitations from above on the values of the vibrational quantum number n at fixed laser intensity I and limitations from below on the values of I at fixed n. In particular, as follows from numerical data of Table I, in the lattice with the red MWL $\lambda^r_m=813.42727$ nm and the laser intensity $I=10\,\mathrm{kW/cm^2}$ the potential wells (10) may host states with $n\leqslant 6$, but the contribution of anharmonic term of (11) does not exceed $\Omega/10$ only for states with $n\leqslant 2$ and achieves the value of 0.8Ω in the highest state $n=6$. For $I=100\,\mathrm{kW/cm^2}$ the potential wells (10) host states with $n\leqslant 21$, and the contribution of anharmonic term is below $\Omega/10$ only for states with $n\leqslant 4$, whereas for states $n>13$ the anharmonic correction exceeds Ω.

Evidently, the intensity-independent part of the anharmonic shift only deepens the trapping potential energy, lowers down vibrational levels and does not influence the clock frequency, if the atom does not change its vibrational state ($\Delta n = 0$) during transition between the ground and excited clock levels.

III. MWL IN A STANDING WAVE

The linear in I, n-independent term of the vibrational energy (11) is determined by only the E1 polarizability, whereas the harmonic and anharmonic coefficients include the difference (8) of the E1 and multipole polarizabilities. Evidently, the principal goal of tuning lattice to the MWL is to make equal the energies (11) for the clock states.

Neglecting the quadratic terms βI^2, the "atomic-motion-insensitive" MWL $\lambda_m = 2\pi c/\omega_m$ may be determined by the equality [13]

$$\alpha_g^{dqm}(\omega_m) = \alpha_e^{dqm}(\omega_m) \equiv \alpha_m^{dqm}. \tag{12}$$

Then eigenfrequencies of vibrational motion for the ground-state and excited atom are equalized and may be written as follows:

$$\Omega_g = \Omega_e = \Omega_m^{(0)}\sqrt{I}, \quad \text{where} \quad \Omega_m^{(0)} = \sqrt{\frac{2\alpha_m^{dqm}k^2}{\mathcal{M}}}. \tag{13}$$

As was mentioned above, the eigenfrequency (13) is proportional to the square root of the laser intensity. In terms of recoil energy the intensity-independent factor may be written as

$$\Omega_m^{(0)} = 2\sqrt{\alpha_m^{dqm}\mathcal{E}^{\rm rec}}. \tag{14}$$

Thus, neglecting the multipole and hyperpolarizability terms, the vibrational frequency (13) may be determined as twice the geometric mean of the lattice potential depth $|U^L_{g(e)}(X=0)| = \alpha^{E1}I$ and the the photon recoil energy.

Equation (12) eliminates the atomic-motion-related clock-frequency dependence on the laser intensity in the lowest order in I. In this case, however, the linear in I shift between bottoms of potentials for ground-state and excited atom remains, due to the difference between dipole polarizabilities at the magic frequency, as is seen from Eqs. (8) and (12)

$$\Delta\alpha_m^{E1} \equiv \alpha_e^{E1}(\omega_m) - \alpha_g^{E1}(\omega_m) = \Delta\alpha_m^{qm}. \tag{15}$$

This difference may be taken into account if the uniform distribution of intensity for all atoms trapped in lattice sites is provided. Correspondingly, the difference between the ground-state and excited-state hyperpolarizabilities, $\Delta\beta_m = \beta_e(\omega_m) - \beta_g(\omega_m)$ determines the second-order shift, which appears both in position-independent and position-dependent terms of the lattice-induced potentials (10) and vibrational energies (11). Assuming the equality (12), the clock frequency shift, related with the difference between vibrational energies for excited and ground-state atom, is

$$\begin{aligned}\Delta\nu_{cl} &= E_e^{\rm vib}(I,n) - E_g^{\rm vib}(I,n)\\ &= a_1(n)I + a_{3/2}(n)I^{3/2} + a_2 I^2,\end{aligned} \tag{16}$$

where coefficients a are determined by the dipole and multipole dynamic polarizabilities, their differences (8), (15) and differences between hyperpolarizabilities of clock levels at the magic wavelength; a_1 and $a_{3/2}$ depend also on the vibrational quantum number n. Assuming identical n for the ground-state and excited atom,

$$\begin{aligned}a_1^{l(c)}(n) &= -\Delta\alpha_m^{qm} - \frac{3\Delta\beta_m^{l(c)}k^2}{4\mathcal{M}\alpha_m^{dqm}}(n^2+n+1/2);\\ a_{3/2}^{l(c)}(n) &= \frac{\Delta\beta_m^{l(c)}k}{\sqrt{2\alpha_m^{dqm}\mathcal{M}}}(n+1/2); \quad a_2^{l(c)} = -\Delta\beta_m^{l(c)}.\end{aligned} \tag{17}$$

The superscripts $l(c)$ appear due to the dependence of hyperpolarizability on polarization [17,21] and correspond to the linear (circular) polarization of the lattice wave. Due to the square-root dependence of the vibrational frequency (13), the half-integer power 3/2 of intensity appears in the shift of the clock frequency (16). In addition, the hyperpolarizability from the anharmonic part of potential provides n-dependent contribution to the linear in I term. These contributions may be written in terms of the the vibrational frequency (13) or the recoil energy (1), as follows:

$$\begin{aligned}a_1^{l(c)}(n) &= -\Delta\alpha^{qm} - \frac{3\Delta\beta_m^{l(c)}\mathcal{E}^{\rm rec}}{2\alpha_m^{dqm}}(n^2+n+1/2)\\ &= -\Delta\alpha^{qm} - \frac{3\Delta\beta_m^{l(c)}\left(\Omega_m^{(0)}\right)^2}{8\left(\alpha_m^{dqm}\right)^2}(n^2+n+1/2);\\ a_{3/2}^{l(c)}(n) &= \Delta\beta_m^{l(c)}\sqrt{\frac{\mathcal{E}^{\rm rec}}{\alpha_m^{dqm}}}(n+1/2) = \frac{\Delta\beta_m^{l(c)}\Omega_m^{(0)}}{2\alpha_m^{dqm}}(n+1/2).\end{aligned} \tag{18}$$

So, all the three coefficients in (16) include the difference between hyperpolarizabilities $\Delta\beta_m$ of the clock levels. The numerical data for susceptibilities of Sr atoms in the red-detuned and blue-detuned magic lattices are presented in Table I. From these data one can derive the following values of coefficients in Eq. (16) for the oscillation number $n = 0$ in linearly polarized lattice:

$$a_1^l = 6.82\frac{\rm mHz}{\rm kW/cm^2}, \quad a_{3/2}^l = -0.192\frac{\rm mHz}{(\rm kW/cm^2)^{3/2}}. \tag{19}$$

TABLE I. Numerical values of E1 polarizabilities, differences between E2-M1 polarizabilities and hyperpolarizabilities [for linear (l) and circular (c) lattice-wave polarization] calculated in the model potential approximation [21], oscillator frequencies and recoil energies for ^{87}Sr atoms in optical lattices with red-detuned (λ_m^r = 813.42727 nm [2]) and blue-detuned (λ_m^b = 389.889 nm [14]) magic wavelengths.

λ_m	813.42727 nm	389.889 nm
α_m^{E1}, $\frac{\rm kHz}{\rm kW/cm^2}$	64.5	−92.7
$\Delta\alpha_m^{qm}$, $\frac{\rm mHz}{\rm kW/cm^2}$	−6.75	−13.6
$\mathrm{Re}\{\Delta\beta_m^l\}$, $\frac{\rm mHz}{(\rm kW/cm^2)^2}$	−1.66	1.15
$\mathrm{Im}\{\Delta\beta_m^l\}$, $\frac{\rm s^{-1}}{(\rm kW/cm^2)^2}$	0	1.56×10^{-5}
$\mathrm{Re}\{\Delta\beta_m^c\}$, $\frac{\rm mHz}{(\rm kW/cm^2)^2}$	−2.43	1.55
$\mathrm{Im}\{\Delta\beta_m^c\}$, $\frac{\rm s^{-1}}{(\rm kW/cm^2)^2}$	0	1.49×10^{-5}
$\Omega_m^{(0)}$, $\frac{\rm kHz}{\sqrt{\rm kW/cm^2}}$	29.9	74.8
$\mathcal{E}^{\rm rec}$, kHz	3.47	15.1

Also, for the circular polarization

$$a_1^c = 6.85\frac{\text{mHz}}{\text{kW/cm}^2}, \quad a_{3/2}^c = -0.282\frac{\text{mHz}}{(\text{kW/cm}^2)^{3/2}}. \quad (20)$$

The value of $a_2^{l(c)} = -\Delta\beta_m^{l(c)}$ may be taken directly from Table I.

Equation (16) together with the data (19) and (20) demonstrates that at the laser intensity around $I = 10\ \text{kW/cm}^2$ the principal contribution to the lattice-induced shift (16) comes from the I^2 term, determined by the net hyperpolarizability $\Delta\beta_m^{l(c)}$. Therefore, to reduce the uncertainty of the shift (16) to the level below 5 mHz, sufficient for the fractional clock uncertainty below 10^{-17}, a precise control of the lattice intensity should be done, with possible deviations not exceeding 1% over the region of trapped atoms. The lattice-induced-shift uncertainty below 0.5 mHz, required for the clock fractional uncertainty at the level of 10^{-18} may be provided by reducing the fractional uncertainties of the laser intensity to 0.1%. The intensity of $I = 10\ \text{kW/cm}^2$ provides the depth of the red-detuned MWL lattice wells

$$\left|U_0^L\right| = \alpha_m^{E1} I \approx 31\ \mu\text{K} \approx 188\mathcal{E}^{\text{rec}} \approx 6.9\Omega_m,$$

quite sufficient for trapping atoms cooled to 1 μK into the lowest vibrational states.

IV. DETERMINATION OF MOTION-INSENSITIVE MWL FROM THE MWL FOR A TRAVELING WAVE

A MWL for a traveling wave (TW) may be determined by measuring the clock shifts of atoms exposed to the TW of a small intensity $I_t < 10^{-3} I$, as experimentally demonstrated in Ref. [14]. To avoid the Doppler and recoil shifts, atoms were trapped in a lattice tuned to a magic frequency ω_m. Evidently, in this case the linear in I_t shift of the clock frequency, caused by the difference of the TW-induced shifts of the clock levels, is determined by the difference of polarizabilities at the TW frequency $\Delta\alpha(\omega_t) = \alpha_e(\omega_t) - \alpha_g(\omega_t)$. The contribution to linear in I_t term comes also from the bilinear in I and I_t term of the fourth-order perturbation theory for the energy of atom in the field of two different monochromatic waves [21,23]. This contribution may be considered as the dependence of polarizabilities on the lattice laser intensity I, determined by the dichromatic hyperpolarizability $\beta_{g(e)}^d(\omega_m,\omega_t)$,

$$\alpha_{g(e)}(\omega_t, I) = \alpha_{g(e)}(\omega_t) + \beta_{g(e)}^d(\omega_m,\omega_t) I.$$

The determination of the MWL for the TW is performed by finding the frequency $\omega_t = \omega_m^t$ for which the clock frequency does not depend on I_t.

Numerical estimates give an approximate equality for order of magnitudes of the monochromatic and dichromatic hyperpolarizabilities, $\beta_{g(e)}(\omega_m)$ and $\beta_{g(e)}^d(\omega_m,\omega_t)$. So the contribution of the bilinear term is on the order of the ratio $I_t/I < 10^{-3}$ (the value of Ref. [14]) in comparison with the quadratic in I term of Eqs. (9)–(11). Thus, the lattice-TW cross effect is less important than the lattice hyperpolarizability effect and therefore does not influence the precision of the MWL measurements. In the following, we confine ourselves to discussion of the uncertainties in the lattice-induced shifts and of the corrections, which should be made to tune the lattice-wave frequency to the motion-insensitive value when the TW is used for determination of the MWL.

Since the spatial distributions of the dipole and multipole interactions (6) for a TW are uniform, the corresponding Stark shifts of the clock levels are position independent. At low TW intensity I_t, the principal contribution to the Stark shifts are given by the sum of dipole and multipole polarizabilities, both proportional to I_t, by neglecting the nonlinear terms. So the MWL in a TW $\lambda_m^t = 2\pi c/\omega_m^t$ may be determined from the equality

$$\alpha_g^{\Sigma}(\omega_m^t) = \alpha_e^{\Sigma}(\omega_m^t) \equiv \alpha_m^{\Sigma}, \quad (21)$$

where

$$\alpha_m^{\Sigma} = \alpha_{g(e)}^{E1}(\omega_m^t) + \alpha_{g(e)}^{qm}(\omega_m^t) \quad (22)$$

is the sum of E1, E2, and M1 polarizabilities.

After having been determined according to Eq. (21), by equalizing clock-level shifts in atoms exposed to a TW, the so determined MWL may be used for a standing wave of an optical lattice. In this lattice, an opposite to (15) relation holds

$$\Delta\alpha_m^{E1} = -\Delta\alpha_m^{qm}. \quad (23)$$

In addition, the combined polarizabilities determining the frequencies of vibrations (13), in the case of equality (21), also differ for upper and lower clock-state atom, as follows:

$$\Delta\alpha_m^{dqm} = -2\Delta\alpha_m^{qm}. \quad (24)$$

So, the difference between frequencies of oscillations inside the lattice site for ground-state and excited atom is

$$\Delta\Omega_m = \Omega_e - \Omega_g = -\Delta\alpha_m^{qm} k\sqrt{\frac{2I}{\alpha_m^{\Sigma}\mathcal{M}}}. \quad (25)$$

This difference imparts an additional term to the right-hand side of Eq. (16), which is proportional to the square root of intensity

$$\Delta\nu_{cl}(n,I) = b_{1/2}(n)I^{1/2} + b_1(n)I + b_{3/2}(n)I^{3/2} + b_2 I^2, \quad (26)$$

where

$$b_{1/2}(n) = -\Delta\alpha_m^{qm}\sqrt{\frac{2k^2}{\alpha_m^{\Sigma}\mathcal{M}}}\left(n+\frac{1}{2}\right) = -2\Delta\alpha_m^{qm}\sqrt{\frac{\mathcal{E}^{\text{rec}}}{\alpha_m^{\Sigma}}}\left(n+\frac{1}{2}\right), \quad (27)$$

and the remaining coefficients in the right-hand side of (26) look similar to (17) and (18) with the replacement of $-\Delta\alpha_m^{qm}$ and α_m^{dqm} by $\Delta\alpha^{qm}$ and α_m^{Σ}, respectively,

$$b_1^{l(c)}(n) = \Delta\alpha^{qm} - \frac{3\Delta\beta_m^{l(c)}\mathcal{E}^{\text{rec}}}{2\alpha_m^{\Sigma}}\left(n^2+n+\frac{1}{2}\right);$$
$$b_{3/2}^{l(c)}(n) = \Delta\beta_m^{l(c)}\sqrt{\frac{\mathcal{E}^{\text{rec}}}{\alpha_m^{\Sigma}}}\left(n+\frac{1}{2}\right); \quad b_2^{l(c)} = -\Delta\beta_m^{l(c)}. \quad (28)$$

With the use of the data of Table I, we have

$$b_{1/2} = 3.13\left(n+\frac{1}{2}\right)\ \text{mHz}/\sqrt{\text{kW/cm}^2};$$
$$b_1^l(n=0) = -6.68\ \text{mHz}/(\text{kW/cm}^2);$$
$$b_1^c(n=0) = -6.65\ \text{mHz}/(\text{kW/cm}^2). \quad (29)$$

With seven-digit accuracy, $b_{3/2}^{l(c)}(n) \approx a_{3/2}^{l(c)}(n)$, whereas an equality $b_2^{l(c)} = a_2^{l(c)}$ holds exactly.

Thus, the definition of the MWL on atoms in a lattice [Eq. (12)] and in a traveling wave [Eq. (21)] differs by the term $\propto \sqrt{I}$ in the lattice-induced shifts of Eqs. (16) and (26).

The term $\propto I^{1/2}$ was first predicted in Ref. [15]. However, the considerations of Ref. [15] were based on an assumption of equality $\alpha_e^{E1}(\omega_m) = \alpha_g^{E1}(\omega_m)$, without account for the contribution of E2-M1 polarizability of Eq. (22). Therefore, the right-hand side of (23) was assumed to be equal to zero and the analytical and numerical results of Ref. [15] did not refer either to standing-wave (12) or to traveling-wave (21) measurements of the MWL.

In addition to the difference between equations for determining the MWL in a standing wave and in a traveling wave, the above considerations bring to evidence a possibility for measuring the contribution of the E2 and M1 interactions and the net polarizability $\Delta\alpha_m^{qm}$ from the difference between MWL values determined in traveling-wave (λ_m^t) and standing-wave (λ_m^s) experiments. So, the difference between the magic frequency determined in a traveling wave, $\nu_m^t = c/\lambda_m^t$, and the magic frequency in a standing wave, $\nu_m^s = c/\lambda_m^s$, may be calculated from Eqs. (12) and (21) as

$$\Delta\nu_m^{ts} = \nu_m^t - \nu_m^s = -\left.\frac{2\Delta\alpha_m^{qm}}{\partial\alpha_e^{E1}(\omega)/\partial\omega - \partial\alpha_g^{E1}(\omega)/\partial\omega}\right|_{\omega=\omega_m}. \tag{30}$$

In particular, with the use of the data of Table I this difference evaluates to $\Delta\nu_m^{ts} = 20.5$ MHz. Subtraction of this value from the magic frequency ν_m^t, measured in a traveling wave, determines the magic frequency ν_m^s for the motion-insensitive optical lattice. The uncertainties of this value do not exceed 10%, coming from the uncertainties of the single-electron model potential approximation in divalent atoms [21] and from approximations in evaluating the frequency derivatives of the dipole polarizabilities.

V. REPULSIVE POTENTIAL IN A LATTICE WITH A BLUE-DETUNED MWL

The potential wells of a lattice with a red-detuned wavelength are replaced by potential barriers in a lattice with blue-detuned wavelength, since the dipole polarizability at the high-frequency wing of resonance line becomes negative. So, in a lattice with a blue-detuned wavelength, atoms are trapped at the nodes of the lattice standing wave. In this case the origin of the coordinate axis X in Eq. (4) should be related with the node, near which the trapped atom oscillates. Then the electric-dipole and multipole parts of interaction (4) exchange their positions and the spatial part (5) is modified to

$$\hat{V}(X) = \hat{V}_{E1}\sin(kX) + (\hat{V}_{M1} + \hat{V}_{E2})\cos(kX). \tag{31}$$

Correspondingly, the second-order and fourth-order in $\hat{V}(X)$ shifts (7) and (9) of atomic energy levels transform to

$$U_{g(e)}^{(2)}(X) = -\left\{\alpha_{g(e)}^{dqm}(\omega)\sin^2(kX) + \alpha_{g(e)}^{qm}(\omega)\right\}I, \tag{32}$$

and

$$U_{g(e)}^{(4)}(X) = -\beta_{g(e)}(\omega)I^2\sin^4(kX), \tag{33}$$

Resolving the sine function in power series of its argument and confining ourselves to harmonic and the lowest-order anharmonic terms, we get the Stark potential for the blue-detuned lattice

$$\begin{aligned} U_{g(e)}^{L(b)}(X) &= U_{g(e)}^{(2)}(X) + U_{g(e)}^{(4)}(X) \\ &= -\alpha_{g(e)}^{qm}(\omega)I - \alpha_{g(e)}^{dqm}(\omega)I(kX)^2 \\ &\quad + \left[\tfrac{1}{3}\alpha_{g(e)}^{dqm}(\omega)I - \beta_{g(e)}(\omega)I^2\right](kX)^4. \end{aligned} \tag{34}$$

In contrast with the red-detuned-wavelength lattice [see (10)], the hyperpolarizability term does not appear either in the constant (position-independent) or the harmonic part ($\propto X^2$) of the potential (34). The anharmonic term is the first instance where the hyperpolarizability appears. So, the quadratic in I corrections to the lattice-induced clock-frequency shift are significantly suppressed due to smallness of anharmonic lattice-atom interaction. Numerical estimates demonstrate that this suppression at $I = 10\text{kW/cm}^2$ achieves nearly two orders of magnitude and falls down with the growth of I due to corresponding fall-down of the anharmonic effects, together with contraction of the oscillator length scaling factor $X_0 = \sqrt{1/\mathcal{M}\Omega_m} \propto I^{-1/4}$.

The bottoms of potential wells [the X-independent terms of (34)] depend on the multipole polarizabilities, which are seven orders smaller than the E1 polarizability (see Table I). Therefore, the principal contributions into the lattice-induced shifts of the clock levels

$$\begin{aligned} E_{g(e)}^{\text{vib}} &\equiv \langle n|\frac{\hat{P}^2}{2\mathcal{M}} + U_{g(e)}^{L(b)}(X)|n\rangle \\ &= -\alpha_{g(e)}^{qm}(\omega)I + \Omega_{g(e)}\left(n+\frac{1}{2}\right) \\ &\quad - \frac{\mathcal{E}^{\text{rec}}}{2}\left[1 - \frac{3\beta_{g(e)}(\omega)I}{\alpha_{g(e)}^{dqm}(\omega)}\right]\left(n^2+n+\frac{1}{2}\right), \end{aligned} \tag{35}$$

comes from the energy of harmonic vibrations, determined by the eigenfrequencies

$$\Omega_{g(e)} = \Omega_{g(e)}^{(0)}\sqrt{I}, \quad \Omega_{g(e)}^{(0)} = 2\sqrt{-\alpha_{g(e)}^{dqm}(\omega)\mathcal{E}^{\text{rec}}}. \tag{36}$$

Similar to (11), the intensity-independent shift here also appears as a result of averaging the linear in intensity anharmonic term of (34).

Thus, the lattice-induced clock frequency shift $\Delta\nu_{cl}$ determined by the difference between energies (35), includes only square-root and linear in I terms

$$\Delta\nu_{cl}(n,I) = E_e^{\text{vib}} - E_g^{\text{vib}} = c_{1/2}(n)I^{1/2} + c_1^{l(c)}(n)I, \tag{37}$$

where (assuming identical vibrational quantum numbers n in clock states)

$$\begin{aligned} c_{1/2}(n) &= \left(\Omega_e^{(0)} - \Omega_g^{(0)}\right)\left(n+\frac{1}{2}\right); \\ c_1^{l(c)}(n) &= -\Delta\alpha^{qm}(\omega) + \frac{3}{2}\mathcal{E}^{\text{rec}}\left[\frac{\beta_e^{l(c)}(\omega)}{\alpha_e^{dqm}(\omega)} - \frac{\beta_g^{l(c)}(\omega)}{\alpha_g^{dqm}(\omega)}\right] \\ &\quad \times \left(n^2+n+\frac{1}{2}\right). \end{aligned} \tag{38}$$

The condition (12) for atomic-motion-insensitive MWL in a standing wave ensures the equality $\Omega_e^{(0)} = \Omega_g^{(0)}$, which cancels out the lowest-order term from (37), as $c_{1/2} = 0$, and the lattice-induced shift (37) remains a linear function, directly proportional to the laser intensity

$$\Delta\nu_{cl}(n, I) = c_1^{l(c)}(n) I, \tag{39}$$

with coefficient

$$c_1^{l(c)}(n) = -\Delta\alpha_m^{qm} + \frac{3\Delta\beta_m^{l(c)}}{2\alpha_m^{dqm}}\mathcal{E}^{\rm rec}\left(n^2 + n + \frac{1}{2}\right). \tag{40}$$

For the lowest vibrational state $n = 0$ of ^{87}Sr atoms in a lattice with the blue MWL $\lambda_m = 389.889$ nm the data of Table I gives $\mathrm{Re}(c_1^l) = 13.48$ mHz/(kW/cm^2), where the contribution of hyperpolarizability [second term in (40)] is below 1%; for the state $n = 2$ we have $\mathrm{Re}(c_1^l) = 11.8$ mHz/(kW/cm^2), and the absolute value of the hyperpolarizability-dependent term amounts to about 14% of $|\Delta\alpha_m^{qm}|$. The contributions to the clock frequency shift come from the real part of hyperpolarizability, whereas the imaginary part (see Table I) determines the rate of two-photon ionization by the lattice wave from the clock states. It is interesting to note that the real part of the hyperpolarizability of the excited $^3P_0$ state exceeds that of the ground state $^1S_0$ by more than two orders of magnitude, while the imaginary part of the ground-state hyperpolarizability is more than three times that of the excited state, in accord with general regularities for the ionization cross section dependence on the free-electron energy (see for example [24]). However, since the contribution of hyperpolarizability in the energy of vibrations (35) comes from the anharmonic term of the Stark potential (34), it is suppressed by the factor $|\mathcal{E}^{\rm rec}/\alpha_m^{dqm} I|$. So, $\mathrm{Im}(c_1^l) = 0.96 \times 10^{-6}(n^2 + n + 1/2)$ s^{-1}/(kW/cm^2) and the total rate of the two-photon ionization is linearly dependent on the laser intensity. For the ground vibrational state $n = 0$ at $I = 10$ kW/cm^2 this rate does not exceed 10^{-5} s^{-1}.

However, when the MWL is determined in a traveling wave, according to Eqs. (21) and (22), the eigenfrequencies of an atom in the upper and lower clock states differ by $\Delta\Omega_m = \Omega_e(\omega_m) - \Omega_g(\omega_m) = 2c_{1/2}(n = 0)\sqrt{I}$, with

$$c_{1/2}(n) = -\frac{\Delta\alpha_m^{qm}}{\alpha_m^{\Sigma}}\Omega_m^{(0)}\left(n + \frac{1}{2}\right),$$
$$\Omega_m^{(0)} = 2\sqrt{-\alpha_{g(e)}^{\Sigma}(\omega)\mathcal{E}^{\rm rec}}.$$

From the data of Table I we have:

$$c_{1/2}(n) = -10.97\left(n + \frac{1}{2}\right)\frac{\rm mHz}{\sqrt{\rm kW/cm^2}}.$$

These data may be useful not only for estimating fractional uncertainties of the clock-frequency measurements, but also for determining experimentally E2-M1 polarizability of the clock transition at the MWL.

With the use of Eq. (30), the difference between the magic frequencies determined in traveling and standing waves, for the blue-detuned lattice is evaluated to $\Delta\nu_m^{ts} = 2.66$ MHz.

One should bear in mind the lack of the radial confinement in a 1D lattice of a blue MWL. Nevertheless, the principal result of elimination of nonlinear in the laser intensity terms and suppression of hyperpolarizability effects in a blue-detuned lattice will also remain in a 3D case.

VI. PRECISION FOR THE MWL

Evidently, the lattice-induced shifts determined in Eqs. (16)–(20), (26)–(29), (37)–(40), may not be reduced to zero simultaneously for all trapped atomic oscillators due to different power dependencies of separate terms and to inhomogeneous distribution of the laser intensity over lattice traps. However, the shifts can be reduced to their minimal possible values and then taken into account in experiment. The idea of the MWL pursues this minimization and its first target is to equalize the principal contributions to the Stark shifts of the upper and lower clock levels, basically determined by dipole polarizabilities.

Naturally, the precision for the value of the MWL should ensure the difference between the first-order in I electric-dipole shifts below the hyperpolarizability and multipole effects, which should be taken into account in high-precision measurements of the clock frequency. To this end, the frequency derivatives of the dipole polarizabilities of the clock levels should be known to control the precision of tuning the lattice laser to the magic frequency [14,16].

To reduce clock uncertainties to the level of 10^{-18}, the fractional uncertainties of the lattice-induced shifts of the clock frequency $|\Delta\nu_{cl}| = |E_e^{\rm vib} - E_g^{\rm vib}|$, due to uncertainties $\Delta\omega_m$ of the magic frequency, at the depth of the lattice traps on the order of 0.1 MHz to 1 MHz (4.8 to 48 μK) should not exceed 0.4×10^{-8}–0.4×10^{-9}. The principal contribution to the lattice-induced shift comes from the lowest-order electric dipole interaction. In the red-detuned lattice these contributions are described by the first and third terms in the right-hand side of Eq. (11). So, the lattice-induced uncertainty may be determined numerically by the derivative [16]

$$\frac{\partial\nu_{cl}}{\partial\omega_m} = \frac{\partial\Delta E^{\rm vib}}{\partial\omega_m} = -\frac{\partial\Delta\alpha_m^{E1}}{\partial\omega_m} I + \frac{\partial\Delta\Omega_m^{(0)}}{\partial\omega_m}\sqrt{I}\left(n + \frac{1}{2}\right), \tag{41}$$

where $\Delta\Omega_m^{(0)} = \Omega_e^{(0)} - \Omega_g^{(0)}$. Simple estimates,

$$\frac{\partial\alpha_m^{E1}}{\partial\omega_m} \approx \frac{\alpha_m^{E1}}{\Delta^{\rm res}} \quad \text{and} \quad \frac{\partial\Omega_m^{(0)}}{\partial\omega_m} \approx \Omega_m^{(0)}\left(\frac{1}{2\Delta^{\rm res}} + \frac{1}{\omega_m}\right),$$

(with 15% precision, as is confirmed in numerical calculations) give

$$\frac{\partial\nu_{cl}}{\partial\omega_m} = -\left[\alpha_m^{E1} I - \frac{\Omega_m^{(0)}}{2}\sqrt{I}\left(n + \frac{1}{2}\right)\right]\left(\frac{1}{\Delta_e^{\rm res}} - \frac{1}{\Delta_g^{\rm res}}\right), \tag{42}$$

where $\Delta_{g(e)}^{\rm res} = \omega_{g(e)}^{\rm res} - \omega_m$ is the detuning from the frequency $\omega_{g(e)}^{\rm res}$ of transition to the nearest resonance state, providing principal contribution to the polarizability of the ground-state (excited) atom. For the red-detuned MWL the detuning from resonance of excited clock level $5s5p(^3P_0)$ on $5s6s(^3S_1)$ state is $\Delta_e^{\rm res} = 72.778$ THz, and for the ground state $5s^2(^1S_0)$ the detuning from resonance on $5s5p(^1P_1)$ state is $\Delta_g^{\rm res} = 281.950$ THz. So the derivative (42) may be presented numerically as

$$\frac{\partial\nu_{cl}}{\partial\omega_m} = -10^{-10}\left\{6.575 I - 1.524\sqrt{I}\left(n + \frac{1}{2}\right)\right\}, \tag{43}$$

with the laser intensity I in kW/cm^2. It is evident, that for $I =$ 10 kW/cm^2 the 0.1 MHz precision for the MWL is sufficient to confine the lattice-induced fractional uncertainties on the clock frequency below 10^{-18}.

The principal contribution to the energy shift of clock levels in the lattice with blue-detuned MWL is determined by the energy vibrations described by the second term in the right-hand side of Eq. (35). So, the derivative of the clock frequency shift is here determined by only the last term in the right-hand side of Eq. (41), which may finally be written as the last term in square brackets of Eq. (42). However, here the resonance detuning $\Delta^{\rm res}$ is negative and for the blue MWL $\lambda = 389.889$ nm the detuning from resonance of excited clock level on $5s6d(^3D_1)$ state is $\Delta_e^{\rm res} = -8.39258$ THz, and for the ground state the detuning from resonance on $5s5p(^1P_1)$ state is $\Delta_g^{\rm res} = -118.414$ THz. So the derivative for the clock-frequency-shift dependence on the blue-detuned laser frequency may be presented numerically as

$$\frac{\partial \nu_{cl}}{\partial \omega_m} = -4.14 \times 10^{-9} \sqrt{I} \left(n + \frac{1}{2} \right), \qquad (44)$$

where the laser intensity I is in kW/cm^2. The 0.1 MHz precision for the MWL is required here to provide lattice-induced fractional uncertainties at the level below 10^{-18} for the clock frequency on atoms confined in the blue MWL lattice to the lowest vibrational state $n = 0$. To this end, the lattice laser frequency precision and stability at the intensity $I = 10$ kW/cm^2 should be on the order of $\Delta\omega_m/\omega_m \approx 10^{-10}$, which is well achievable with such as GPS disciplined Rb oscillators.

VII. CONCLUSION

In summary, this paper presents detailed quantitative investigations of the lattice-induced shifts of the clock frequency in Sr atoms, which may not be eliminated in a MWL lattice due to higher-order (hyperpolarizability), multipole (M1-E2), harmonic, and anharmonic [proportional to the second-order (X^2) and fourth-order (X^4) displacement of an atom from its equilibrium position, respectively] effects of the atom-lattice-field interaction. The analysis distinguished between two different methods for determining the MWL: for atoms in a standing wave (12) and for atoms in a traveling wave (21). The resolutions in powers of intensity for the clock-frequency shifts in a lattice with a blue MWL (37) in the indicated approximations include only two terms, $\propto I^{1/2}$ and $\propto I$, whereas in a lattice with a red MWL (16), (26) additional terms appear, $\propto I^{3/2}$ and $\propto I^2$. In the case of exact equalization of the harmonic oscillation frequencies of an atom in its upper and lower clock states, the terms $\propto I^{1/2}$ disappear in Eqs. (16) and (37) for both types (red- and blue-detuned) of lattices.

In a lattice with a red-detuned MWL the anharmonic terms of the lattice potential transfer hyperpolarizability effects into the terms $\propto I$ and $\propto I^{3/2}$. However, the principal contribution to the clock-frequency shift (16) at the laser intensity $I =$ 10 kW/cm^2 is given by the pure hyperpolarizability term, determining the quadratic in I vibrational-state-independent shift of the Stark potential well. The hyperpolarizability-related harmonic effects are linear and anharmonic effects are quadratic in the vibrational quantum number n.

In a lattice with a blue MWL the hyperpolarizability effect appears only in the anharmonic atom-lattice interaction. Therefore it is quadratically dependent on n and contributes only into the linear in I term. For the ground vibrational state, $n = 0$, the contribution of hyperpolarizability to c_1 in (40) and consequently, to the clock-frequency shift, does not exceed 1%.

Significant dependence on the vibrational quantum numbers of coefficients determining the lattice-induced shifts in Eqs. (16) and (39) suggests application of sideband cooling to the vibrational ground state is preferable in prior to spectroscopy. Finally, on the basis of calculated data we can state that high-precision measurement and account of the unavoidable lattice-induced shifts (16), (39), together with high stability of the lattice magic frequency, makes it possible to proceed to the frequency standard on Sr atoms in optical lattices with precision in the eighteenth decimal place. The obtained results provide necessary quantitative information, which can be rather important for the choice of experimental methods to accurately account for the unavoidable shifts of the clock frequency.

Equation (30) indicates the possibility for determining the motion-insensitive MWL from straightforward measurements of the MWL for a traveling wave. Inversely, the difference between the MWL measured in standing and traveling waves provides the possibility to measure the ratio of the net multipole polarizabilities and net frequency derivative of the dipole polarizabilities for the clock states.

ACKNOWLEDGMENTS

V.D.O. was supported by the Russian Foundation for Basic Research (RFBR) Grant No. 11-02-00152-a. A.V.T. and V.I.Yu. were supported by the Ministry of Education and Science of the Russian Federation in the frame of the Program "Scientific and scientific-pedagogical personnel of innovative Russia" (Contract No. 16.740.11.0466 and Agreement No. 8387), by RFBR (Grants No. 12-02-00454, No. 12-02-00403, No. 11-02-00775, and No. 11-02-01240), by the Russian Academy of Sciences (RAS) and the Presidium of Siberian Branch of RAS. H.K. was supported in part by the JSPS through the FIRST Program and by the Photon Frontier Network Program of MEXT, Japan.

[1] A. D. Ludlow, T. Zelevinsky, G. K. Campbell, S. Blatt *et al.*, Science **319**, 1805 (2008).

[2] P. G. Westergaard, J. Lodewyck, L. Lorini, A. Lecallier, E. A. Burt, M. Zawada, J. Millo, and P. Lemonde, Phys. Rev. Lett. **106**, 210801 (2011).

[3] T. Akatsuka, M. Takamoto, and H. Katori, Nature Phys. **4**, 954 (2008).

[4] C. Lisdat, J. S. R. Vellore Winfred, T. Middelmann, F. Riehle, and U. Sterr, Phys. Rev. Lett. **103**, 090801 (2009).

[5] L. Yi, S. Mejri, J. J. McFerran, Y. Le Coq, and S. Bize, Phys. Rev. Lett. **106**, 073005 (2011).
[6] J. A. Sherman, N. D. Lemke, N. Hinkley, M. Pizzocaro, R. W. Fox, A. D. Ludlow, and C. W. Oates, Phys. Rev. Lett. **108**, 153002 (2012).
[7] D. Meiser, J. Ye, D. R. Carlson, and M. J. Holland, Phys. Rev. Lett. **102**, 163601 (2009).
[8] J. Lodewyck *et al.*, Trans. Ultrason. **59**, 411 (2012).
[9] V. D. Ovsiannikov, A. Derevianko, and K. Gibble, Phys. Rev. Lett. **107**, 093003 (2011).
[10] V. I. Yudin, A. V. Taichenachev, M. V. Okhapkin, S. N. Bagayev, and Chr. Tamm, E. Peik, N. Huntemann, T. E. Mehlstaubler, and F. Riehle, Phys. Rev. Lett. **107**, 030801 (2011).
[11] T. Middelmann, S. Falke, C. Lisdat, and U. Sterr, Phys. Rev. Lett. **109**, 263004 (2012).
[12] M. AS. Safronova, S. G. Porsev, U. I. Safronova, M. G. Kozlov, and C. W. Clark, Phys. Rev. A **87**, 012509 (2013).
[13] H. Katori, K. Hashiguchi, E. Yu. Il'inova, and V. D. Ovsiannikov, Phys. Rev. Lett. **103**, 153004 (2009).
[14] M. Takamoto, H. Katori, S. I. Marmo, V. D. Ovsiannikov, and V. G. Pal'chikov, Phys. Rev. Lett. **102**, 063002 (2009).
[15] A. V. Taichenachev, V. I. Yudin, V. D. Ovsiannikov, V. G. Pal'chikov, and C. W. Oates, Phys. Rev. Lett. **101**, 193601 (2008).
[16] H. Katori, M. Takamoto, V. G. Pal'chikov, and V. D. Ovsiannikov, Phys. Rev. Lett. **91**, 173005 (2003).
[17] A. V. Taichenachev, V. I. Yudin, V. D. Ovsiannikov, and V. G. Pal'chikov, Phys. Rev. Lett. **97**, 173601 (2006).
[18] Z. W. Barber, J. E. Stalnaker, N. D. Lemke, N. Poli, C. W. Oates, T. M. Fortier, S. A. Diddams, L. Hollberg, C. W. Hoyt, A. V. Taichenachev, and V. I. Yudin, Phys. Rev. Lett. **100**, 103002 (2008).
[19] A. Brusch, R. Le Targat, X. Baillard, M. Fouché, and P. Lemonde, Phys. Rev. Lett. **96**, 103003 (2006).
[20] P. Lemonde and P. Wolf, Phys. Rev. A **72**, 033409 (2005).
[21] N. L. Manakov, V. D. Ovsiannikov, and L. P. Rapoport, Phys. Rep. **141**, 319 (1986).
[22] D. A. Varshalovich, A. N. Moskalev, and V. K. Khersonsky, *Quantum Theory of Angular Momentum* (World Scientific, Singapore, 1988).
[23] A. G. Fainstein, N. L. Manakov, V. D. Ovsiannikov, and L. P. Rapoport, Phys. Rep. **210**, 111 (1992).
[24] V. D. Ovsiannikov, I. L. Glukhov, and E. A. Nekipelov, J. Phys. B **45**, 095003 (2011).